Biophysical Chemistry, 48 (1993) 49–59
Elsevier Science Publishers B.V., Amsterdam

BIOCHE 01787

Tryptophan fluorescence quenching in rabbit skeletal myosin rod

Yoke-chen Chang and Richard D. Ludescher *

Department of Food Science, Rutgers University and the New Jersey Agricultural Experiment Station, Cook College, New Brunswick, NJ 08903 (USA)

(Received 2 April 1993; accepted in revised form 12 May 1993)

Abstract

The solvent accessibility of the four tryptophans of rabbit skeletal muscle myosin rod was investigated using steady-state and time-resolved fluorescence quenching by iodide, acrylamide, and cesium. The quenching by iodide and acrylamide was biphasic; the discrete, long lifetime component was quenched with bimolecular collision constants (k_q) of 1×10^9 M^{-1} s^{-1} and 1.6×10^9 M^{-1} s^{-1}, respectively, while the Gaussian distributed, short lifetime component was quenched with a k_q value of 0.3×10^9 M^{-1} s^{-1} and 0.04×10^9 M^{-1} s^{-1}, respectively. Comparison with k_q values for *N*-acetyl-tryptophanamide indicated that the fractional solvent accessibility was about 25% for the long and less than 10% for the short lifetime component. Cesium quenching was monophasic and provided evidence of an excess of positive charge around these tryptophans. Our findings cast doubt on the general application of the simple coiled-coil model to describe coiled-coil interactions in this protein in solution.

Keywords: Fluorescence; Lifetime; Tryptophan; Quenching; Protein; Coiled-coil model

1. Introduction

The structure and dynamics of the α-helical coiled-coil, the supersecondary structural motif generated by the left-handed supercoiling of two α-helices, has important implications for the structure of fibrous proteins such as myosin, tropomyosin, and the intermediate filaments [1], for the structure of helical bundles in integral membrane proteins [2], and for the folding interactions that generate helix–helix contacts in globular proteins [2].

In this and a previous study [3] we have used fluorescence from the intrinsic tryptophans of the coiled-coil portion of myosin (called myosin rod when isolated from myosin by proteolysis) to investigate the local structure of the coiled-coil motif in this fibrous protein. The two tryptophans per polypeptide chain (four per rod) are located at equivalent hydrophobic *d* sites in the seven residue (heptad) repeat, $(abcdefg)_n$, found in all coiled-coil amino acid sequences [4,5]. In our previous study [3], we determined that the fluorescence from these residues arises from two populations of tryptophans with different spectral

* *Correspondence to:* Dr. Richard Ludescher, Dept. of Food Science, Rutgers University, P.O. Box 231, Cook College, New Brunswick, NJ 08903-0231.

properties. The major population has a discrete long lifetime with spectral properties characteristic of tryptophan in a polar environment and the minor population has complex, heterogeneous decay kinetics described by a broad Gaussian distribution of short lifetimes with the spectral properties characteristic of tryptophan in a nonpolar environment. In this study we demonstrate that the fluorescence of the discrete long lifetime component is efficiently quenched by addition of the quenchers iodide or acrylamide, and is thus exposed to aqueous solvent, while the fluorescence from the Gaussian distribution short lifetime components is quenched inefficiently by these quenchers and is thus effectively shielded from aqueous solvent. These results suggest that the coiled-coil in solution exists in at least two different conformations, one in which some of the tryptophans at these hydrophobic *d* sites are buried at the coiled-coil interface and another, more probable conformation, in which the tryptophans are at the surface of the coiled-coil exposed to solvent.

2. Materials and methods

2.1. Protein preparations

Myosin was extracted from the skeletal muscle of New Zealand white rabbits as described in reference [3]. The purified myosin was stored at −20°C in myosin buffer (MB: 0.5 *M* KCl, 0.5 m*M* EDTA, 0.5 m*M* dithiothreitol, 20 m*M* MOPS, pH 7.0) [1] that contains 50% glycerol (v/v) as an antifreeze. The myosin rod was prepared from myosin by digestion with α-chymotrypsin (Sigma Chemical Co., St. Louis, MO) at room temperture [3]. The myosin rod was purified from S-1 and undigested myosin by ethanol precipitation [6]. The purity of rod samples was checked by SDS-polyacrylamide gel electrophoresis [7]. The rod preparations that were used to collect the data cited herein all showed one dominant band in 10% polyacrylamide gels. Densitometry of stained gels indicated that the protein was ≥ 95% rod with the remainder smaller fragments. The purified myosin rod was stored at −20°C in MB plus 50% glycerol (as described above).

2.2. Steady-state quenching measurements

Aliquots from freshly prepared stock solutions of KI (ACS grade), acrylamide (electrophoresis grade), or CsCl (optical grade) in MB were added as a quencher to a 1.7 ml sample of myosin rod (0.2 mg/ml) or NATA (10 μM) in myosin buffer at 20°C. All steady-state fluorescence intensity measurements were made on a SPEX F1T11 spectrofluorimeter equipped with temperature controlled sample holder. Quenching measurements were performed using excitation at 290 nm (0.75 nm band pass) and emission at 350 nm (30 nm band pass) for iodide quenching studies, excitation at 300 nm (0.38 nm band pass) and emission at 360 nm (30 nm band pass) for acrylamide, and excitation at 280 nm (0.38 nm band pass) and emission at 340 nm (30 nm band pass) for cesium quenching studies. All fluorescence intensity measurements were corrected for dilution effects. Corrections were made for acrylamide absorption at 300 nm using an extinction coefficient for acrylamide at 300 nm of 0.15 M^{-1} cm^{-1} (maximum adjustment 5% at 1.2 *M* acrylamide). Quenching data at low quencher concentration were plotted as the ratio of the fluorescence intensity in the absence (F_0) to the intensity in the presence (F) of quencher versus the quencher concentration. The quenching curves were fit by linear regression; the fit slope was equated to K_{sv} in the Stern–Volmer equation,

$$F_0/F = 1 + K_{sv}[Q] \quad (1)$$

where [Q] is the concentration of quencher and K_{sv} is the Stern–Volmer quenching constant. $K_{sv} = k_q \tau_0$, where k_q is the bimolecular quenching

[1] Abbreviations: EDTA, ethylenediaminetetraacetic acid; FWHM, full width half maximum; MB, myosin buffer; KDP, potassium dihydrogen phosphate; LMM, light meromyosin; MOPS, 4-morpholinepropanesulfonic acid; NATA, *N*-acetyl-tryptophanamide; NdYAG, neodymium yttrium aluminum garnet; SDS, sodium dodecyl sulfate; S-2, subfragment 2.

constant and τ_0 is the lifetime of rod in the absence of quencher at 20°C. In those cases where the Stern–Volmer plots showed downward curvature, the quenching results were plotted as the ratio F/F_0 and analyzed using the following expression [8]:

$$F/F_0 = \sum_{i=1}^{n} f_i/(1 + K_{sv,i}[Q]) \qquad (2)$$

where f_i is the fractional fluorescence and $K_{sv,i}$ is the Stern–Volmer quenching constant for each component. Data at high concentration of iodide were fit to this equation using the commercial least squares fitting program NFIT (Island Products, Galveston, TX). Equation (2) was modified to account for the possibility of static quenching by including a term in $\exp(V[Q])$ [8].

$$F/F_0 = \sum_{i=1}^{n} f_i/(1 + K_{sv,i}[Q])\exp(V[Q]) \qquad (3)$$

where V is the static quenching constant [9].

2.3. Time-resolved quenching measurements

Lifetime decay measurements were performed on the time-correlated single photon counting fluorimeter at the Regional Laser and Biotechnology Laboratory (RLBL), Department of Chemistry, University of Pennsylvania. The details of the instrument are described in ref. [3]. The lifetime decays of myosin rod were collected as a function of the concentration of the quenchers KI and acrylamide at constant ionic strength by using excitation at 290 nm and emission at 350 nm (bandpass 20 nm). The decays for sets of each quenching data at different quencher concentrations were analyzed simutaneously using global fitting routines on the program Globals Unlimited (University of Illinois) that was developed by Beechem and colleagues [10,11]. This program was used to perform lifetime distribution and discrete lifetime fits simutaneously on multiple data sets. The goodness-of-fit was evaluated by examination of the value of the global χ^2 and plots of the modified residuals and auto-correlation functions for individual data sets. A fit was considered appropriate when the modified residuals and auto-correlation functions showed random deviations about zero and the global χ^2 value was less than 3.

The lifetime components (τ) were plotted as τ_0/τ vs. [Q], where τ_0 is the lifetime in the absence of quencher and τ is the lifetime in the presence of quencher. These plots were analyzed using the Stern–Volmer quenching formalism (eq. 1). τ_0 was also used to calculate the collisional rate constant (k_q) from the Stern–Volmer quenching constant (K_{sv}) in both steady-state and time-resloved quenching studies.

3. Results

3.1. Steady-state quenching

The degree of solvent exposure of the tryptophans in myosin rod was evaluated using collisional quenching with three different quenchers, the negatively charged quencher iodide, the neutral quencher acrylamide, and the positively charged quencher cesium. Typical Stern–Volmer quenching plots for these three quenchers are shown in Fig. 1. The quenching behavior of rod was compared for each quencher with that of *N*-acetyl-tryptophanamide (NATA) which represents the case of tryptophan fully exposed to aqueous solvent; comparison of the quenching behavior of rod to that of NATA allows an estimate of the fractional solvent exposure of the rod tryptophans [12]. At low concentration of iodide, under experimental conditions in which the salt concentration was maintained constant at 0.5 *M* (Fig. 1A), the Stern–Volmer plot of the ratio of the fluorescence intensity in the absence to the intensity in the presence of quencher (F_0/F) was linear with iodide concentration (correlation coefficients ≥ 0.995); Stern–Volmer plots were also linear at low concentrations of acrylamide and cesium (correlation coefficients ≥ 0.995) (Figs. 1B, 1C). The Stern–Volmer quenching constants (K_{sv}) calculated from the slopes of these curves are summarized in Table 1 (low [Q] case). Both acrylamide and iodide efficiently quenched the tryptophan fluorescence of rod with quenching constants of 7.44 and 4.11 M^{-1}, respectively, at

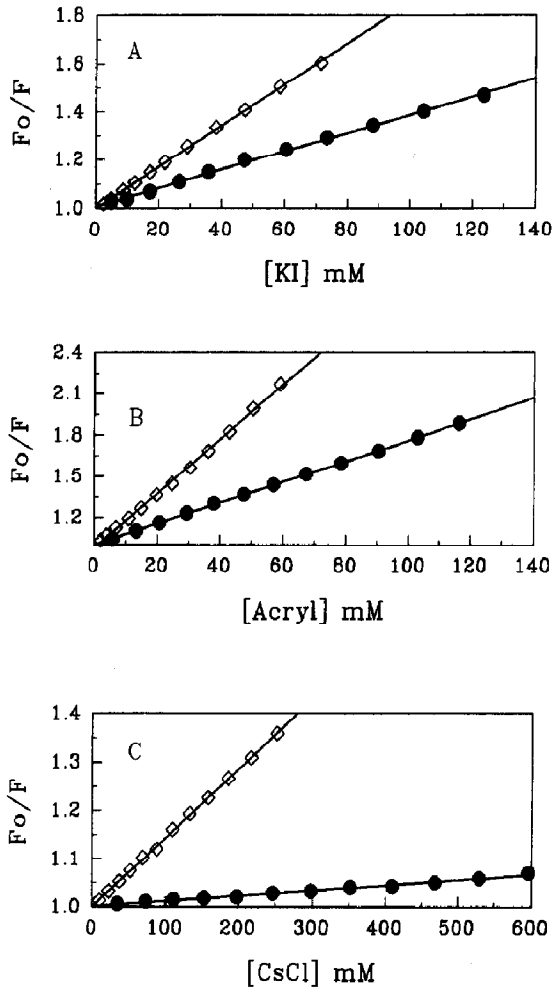

Fig. 1. Stern–Volmer plots of the ratio of the tryptophan fluorescence intensity in the absence (F_0) and presence (F) of quencher for NATA (□) and myosin rod (●) in MB at 20°C. The data are for quenching by potassium iodide (A), acrylamide (B), and cesium chloride (C). Experiments were conducted at low quencher concentrations and, in the case of the charged quenchers, at constant ionic strength.

20°C. These quenching constants are similar to those seen in other soluble proteins with surface accessible tryptophans [8]. The Stern–Volmer constants for cesium quenching of rod and NATA were nearly an order of magnitude smaller than those for iodide and acrylamide because cesium has a quenching efficiency significantly less than unity [13].

At higher concentrations of quencher, in experiments conducted at variable ionic strength in the case of the ionic quenchers, the Stern–Volmer plots were linear for cesium but not for iodide and acrylamide (Fig. 2). The quenching constants from Stern–Volmer analysis of the cesium data at high concentration were essentially the same as those found at low concentration (Table 1). The curvature in the Stern–Volmer plot of iodide, however, suggested that there were at least two populations of tryptophans in the rod with different K_{sv} values [8,14] and thus different accessibilities to iodide and acrylamide. The iodide quenching data were thus analyzed using a two component dynamic quenching model [eq. 2 in Section 2) in order to estimate the different Stern–Volmer quenching constants. Iodide quenching data and a two component fit are plotted as the ratio F/F_0 in Fig. 3A; the Stern–Volmer constants from this two component analysis were 5.29 and 0.305 M^{-1} with fractional amplitudes of 0.83 and 0.17, respectively.

Since the structure of the rod is known to be influenced by ionic strength [15], the effect of

Table 1

Stern–Volmer constants for fluorescence quenching of myosin rod and NATA [a]

Quencher	NATA [b,d]	Myosin rod		
		Intensity [b]		Lifetime [c]
		Low [d] [Q]	High [e] [Q]	
Cesium	1.79	0.119	0.112	–
Acrylamide	19.2	7.44	8.38 [f]	6.18
			≤ 0.0344	≤ 0.5 [g]
Iodide	9.52	4.11	5.29 [f]	4.510
			0.305	≤ 0.4 [g]

[a] Samples at 20°C in MB.
[b] Data from effect of quencher on steady-state intensity at 350 nm.
[c] Data from effect of quencher on magnitude of long (5.4 ns) liftime.
[d] Data from quenching curves at constant ionic strength with low concentration of quencher.
[e] Data from quenching curves at variable ionic strength with high concentration of quencher.
[f] Quenching constants from two component analysis (eq. 2, Section 2) of quenching curves at high concentration of iodide and from two component analysis (eqs. 2 and 3, Section 2) of quenching curves at high concentration of acrylamide.
[g] Estimated (see text for details).

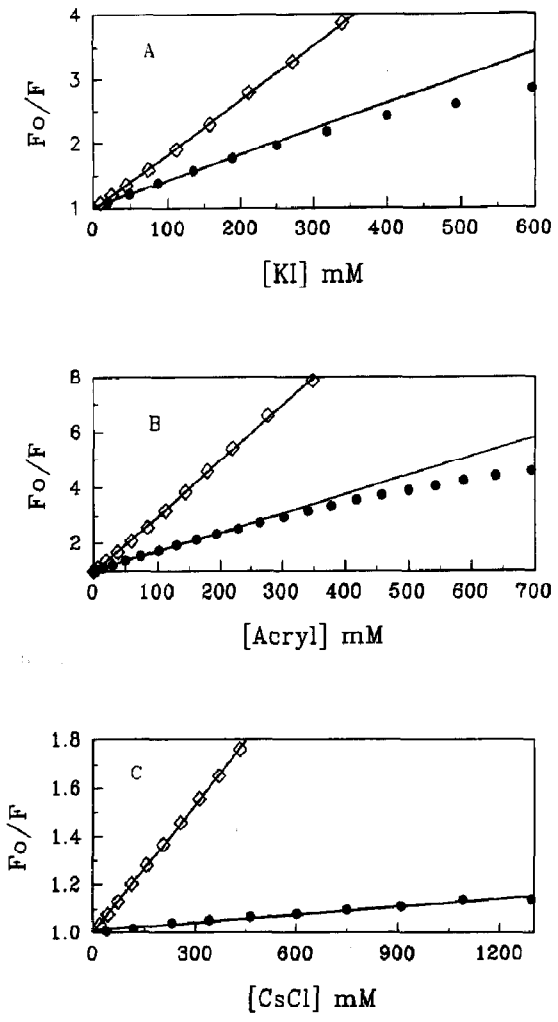

Fig. 2. Stern–Volmer plots of the ratio of the tryptophan fluorescence intensity in the absence (F_0) and presence (F) of quencher for NATA (□) and myosin rod (●) in MB at 20°C. The data are for quenching by potassium iodide (A), acrylamide (B), and cesium chloride (C). Experiments were conducted at high quencher concentrations and, in the case of the charged quenchers, at variable ionic strength.

ionic strength *per se* on the tryptophan fluorescence in rod was investigated by adding KCl to rod samples; the fluorescence intensity remained constant, after correction for the dilution effect, over a concentration range from 0 to 1.35 M KCl (data not shown).

The acrylamide quenching data were analyzed using a two component dynamic quenching model (eq. 2) to estimate the different Stern–Volmer quenching constants for this neutral quencher; these data (plotted as the ratio F/F_0 in Fig. 3B) are well fit with Stern–Volmer constants of 8.38 and $\leq 0.0344\ M^{-1}$ with fractional amplitudes of 0.93 and 0.07, respectively. The same data were also fit using a more complex two-component dynamic–static model (eq. 3); the Stern–Volmer constants from this analysis were similar to those from the simple dynamic model and the static quenching constant (V) was 0 M^{-1}. There was thus no direct evidence for static quenching by acrylamide in the rod.

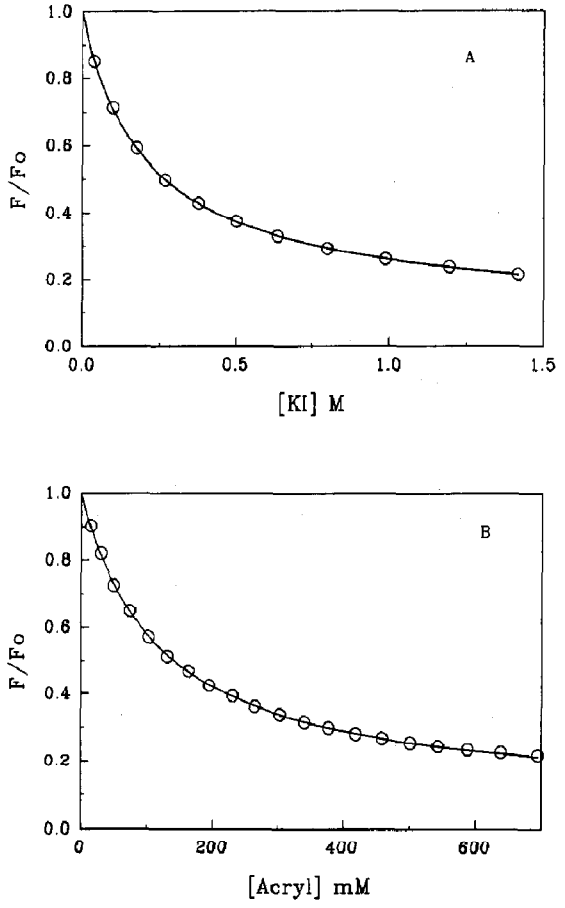

Fig. 3. Quenching of tryptophan fluorescence in myosin rod at 20°C in MB by potassium iodide at variable ionic strength. The data are plotted as the ratio of the fluorescence intensity in the presence (F) to the intensity in the absence (F_0) of quencher. The smooth curve is a two component fit to the data using eq. (2) (Section 2). Details in text and in Table 1.

3.2. Lifetime resolved quenching

The effect of iodide and acrylamide quenching on the individual lifetime components of the rod can provide a more detailed description of solvent quenching in proteins [16–18]. We therefore collected intensity decays of rod fluorescence as a function of quencher concentration for the two efficient quenchers iodide and acrylamide and analyzed the data sets using global fitting procedures [11]. The fluorescence intensity decay of myosin rod at 20°C in MB in the absence of quencher was shown in the previous study [3] to require a discrete long lifetime component and a broad gaussian distribution of short lifetimes for an adequate description. Data sets of intensity decays collected as a function of quencher concentration over the range from 0 to about 200 mM were thus analyzed using a bimodal analysis with a discrete long lifetime and a Gaussian distribution of short lifetimes. The quenching data sets were well fit using a model in which the Gaussian distribution of short lifetimes was linked (constrained to the same values) across all data sets, and the long, discrete lifetime and the amplitudes of all components were allowed to vary across all data sets. The modified residuals from this analysis for individual data sets quenched by iodide are plotted in Fig. 4; the low χ^2 values for these analyses, in the range from 1.13–1.18, and the flat and random residuals plots demonstrate that this model is an excellent description of the data. A similar model was used to fit the acrylamide quenching data; the χ^2 values for these analyses were in the range from 1.05–1.35 and the modified residuals plots (not shown) resembled those shown in Fig. 4.

The global analyses of both iodide and acrylamide quenching thus indicated that only the long lifetime component was efficiently quenched by either iodide or acrylamide. This global analysis agrees with a preliminary study, based on analyses of individual data sets using discrete multiexponential decays, which found that only the long lifetime component was quenched by addition of iodide over the concentration range from 0–210 mM [19].

The lifetime distributions used to analyze the unquenched decay data are plotted in Fig. 5. The data were fit with a discrete long lifetime component of 5.40 ns (fractional amplitude of 0.79) and a broad (1.49 ns FWHM) Gaussian distribution of lifetimes centered at 0.91 ns (fractional amplitude of 0.21). These values are similar to the bimodal distribution values needed to fit the wavelength dependent data described previously [3].

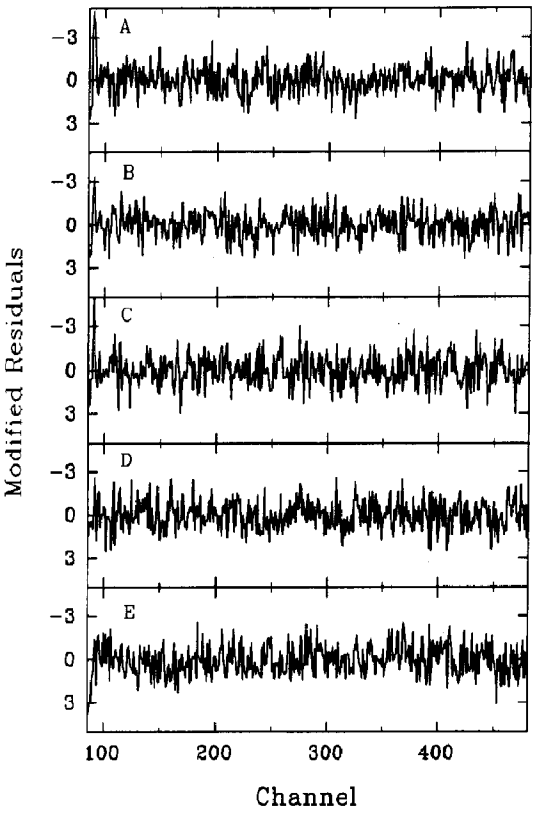

Fig. 4. Modified residuals for global analysis of iodide quenching of rod fluorescence at 20°C in MB using a bimodal model of the quenching behavior. The Gaussian distribution of short lifetimes was linked across all data sets (mean lifetime of 0.91 ns, FWHM of 1.49 ns) and the discrete, long lifetime component and the amplitudes of both components were varied across all the data sets. The residuals plots are for fits to decays in the presence of 0 mM KI (A), 45 mM KI (B), 100 mM KI (C), 154 mM KI (D), and 250 mM KI (E).

The addition of iodide over the concentration range from 0 to 250 mM quenched the long lifetime by over a factor of two (from 5.40 to 2.47 ns). Within the error of our analysis, iodide did not quench the Gaussian distribution of short lifetimes; assuming that the global analysis cannot

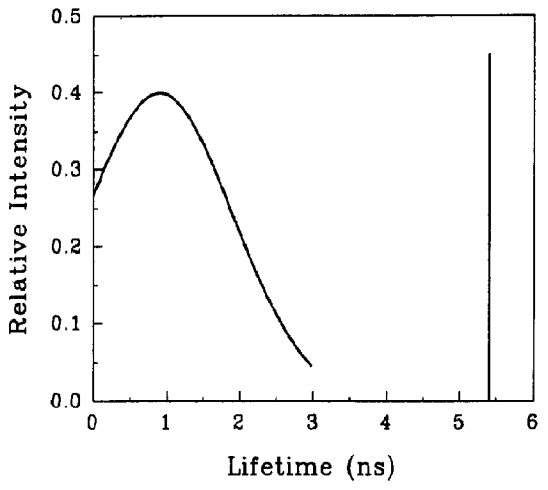

Fig. 5. Distribution of lifetimes used to describe the intensity decay of tryptophan fluorescence in myosin rod at 20°C in MB in the absence of quencher. The normalized amplitudes are 0.79 for the long lifetime and 0.21 for the short lifetime distribution. Further details in text.

detect a decrease of less than 10% in the mean of the short lifetime distribution, we estimate that the Stern–Volmer constant for this species is less than 0.4 M^{-1}. A Stern–Volmer analysis of the ratio of the long lifetimes in the absence to those in the presence of quencher (τ_0/τ) is plotted in Fig. 6A; the plot is linear (correlation coefficient of 0.96) with a slope (K_{sv}) of 4.51 M^{-1} (Table 1). The global analyses indicated that the normalized amplitudes for the discrete long lifetime component remained constant at about 0.79 over the range of quencher concentration from 0 to 100 mM but decreased at higher quencher concentrations (data not shown).

The neutral quencher acrylamide had similar effects on the lifetime components of tryptophan fluorescence in rod. As the concentration of acrylamide increased from 0 to 200 mM the discrete long lifetime was quenched from 5.40 ns to 2.54 ns while the Gaussian distribution of short lifetimes remained unchanged; again, assuming that the global analysis cannot detect a 10% decrease in the mean of the short lifetime distribution, we estimate that the K_{sv} of this component is less than 0.5 M^{-1}. A Stern–Volmer analysis of the quenching of the long lifetime component is plotted in Fig. 6B; this plot is also linear (correlation coefficient of 0.97) with a slope of 6.18 M^{-1} (Table 1). The normalized amplitudes for the discrete long lifetime component also remained constant at about 0.79 over the range of acrylamide concentration from 0 to 80 mM but decreased at higher acrylamide concentrations.

3.3. Bimolecular quenching constants

The Stern–Volmer quenching constant is the product of a bimolecular collision constant (k_q) and the lifetime of the unquenched species [20]. The collision constants for quenching of rod fluorescence by cesium, acrylamide, and iodide, calculated from the quenching constants of Table 1 and the unquenched lifetimes, are summarized in

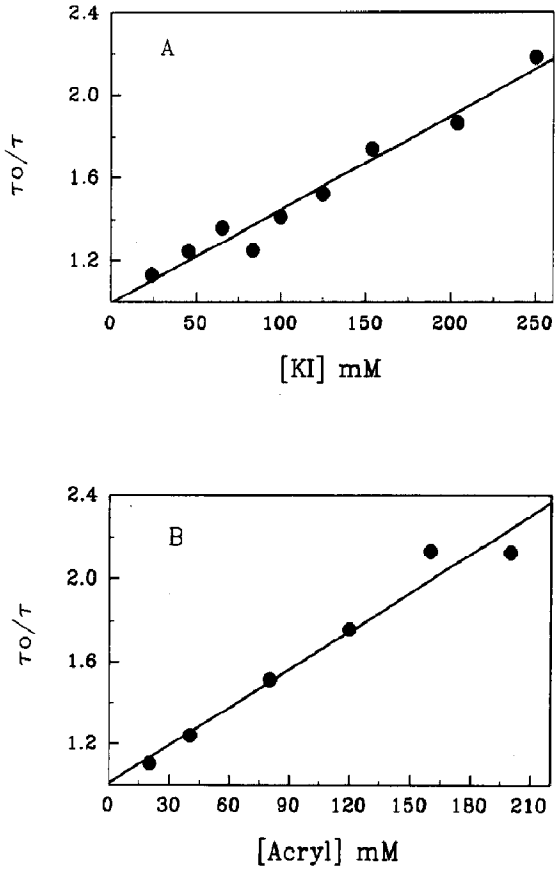

Fig. 6. Stern–Volmer plots of the ratio of the tryptophan long lifetime in the absence (τ_0) and presence (τ) of quencher for potassium iodide (A) and acrylamide (B) quenching of rod at 20°C in MB. The lines are linear least-squares fits to the data. Details in text and in Table 1.

Table 2

Bimolecular collision constants from fluorescence quenching of myosin rod and NATA[a]

Quencher	NATA[b]	Myosin rod		
		Intensity [c]		Lifetime [d]
		Low [Q]	High [Q]	
Cesium	0.597	0.0229	0.0215	–
Acrylamide	6.40	1.43	1.55	1.14
			≤ 0.0378	≤ 0.549
Iodide	3.17	0.791	0.980 [d]	0.835
			0.335 [e]	≤ 0.440

[a] Calculated from the K_{sv} values of Table 1 for samples at 20° in MB.
[b] Calculated using $\tau = 3.0$ ns [21].
[c] Calculated using $\langle\tau\rangle = 5.20$ ns.
[d] Calculate using the value of the long lifetime, $\tau = 5.4$ ns, and the mean of the short lifetime distribution, $\bar{\tau} = 0.91$ ns.
[e] Calculated using the mean lifetime of the Gaussian distribution, $\tau = 0.91$ ns.

Table 2; a value of 3.0 ns [21] was used to calculate k_q for quenching of NATA.

The rate constant for collision of acrylamide with the discrete long lifetime tryptophan species in rod was 1.14×10^9 M^{-1} s^{-1}; this value is in the range found for acrylamide quenching of tryptophan fluorescence in globular proteins but smaller than the maximum value of about 4×10^9 M^{-1} s^{-1} found for quenching of fully solvent exposed tryptophans in proteins [8]. The small difference between the intensity and lifetime values for acrylamide (Table 2) probably reflects the difficulties associated with interpreting the steady-state acrylamide quenching data using a two component dynamic-static quenching model (Section 4). We estimate that the k_q for collision of acylamide with the short lifetime component was less than 0.549×10^9 M^{-1} s^{-1} (Table 2).

The k_q value for collision of iodide with the major (83%) quenching component of rod was 0.980×10^9 M^{-1} s^{-1} based on steady-state quenching data; this value is similar to the rate constant for collision of iodide with the long lifetime component determined from lifetime-resolved quenching (Table 2). The rate constant for collision of iodide with the minor (17%) component was 0.335×10^9 based on the intensity data; this value was in agreement with the estimate of k_q for the short lifetime component based on time-resolved measurements.

The ratio of the collisional rate constant (k_q) of rod to that of NATA for any fluorescent species is a measure of the accessibility of that species to the quencher [12]. These ratios for the discrete, long lifetime component were 0.18 and 0.26 for acrylamide and iodide, respectively. For a protein the size of rod the k_q ratio is about 0.5 for a fully accessible (surface) fluorophore; comparison with modeling data [12] indicated that the fractional accessibility of the long lifetime species to both iodide and acrylamide was about 20–25%. The similarity of these values suggests that the solvent accessibility (that is, fractional solvent exposure) of the long lifetime species was also about 20–25%. The k_q ratio of 0.105 for iodide quenching of the Gaussian distributed short lifetime species indicated that the fractional accessibility of the short lifetime species to iodide calculated from the model [12] was less than 10%.

In the case of cesium, the k_q values for both rod and NATA were small and reflected the inefficient nature of the collisional quenching process for this quencher [13]. The k_q ratio, which adjusts for this inefficiency [8], was only 0.05 indicating efficient shielding (on average) of all tryptophans from this positively charged quencher; this low value suggests [22] that positively charged side chain residues are grouped around some or all of the tryptophans.

4. Discussion

The two pairs of tryptophans in myosin rod are located at hydrophobic *d* sites in the heptad repeat that forms the basis for the coiled-coil structure [23–25]. Extensive model building studies [1,4,26] as well as a recent crystallographic structure of the coiled-coil DNA binding protein GCN4 [27] indicate that coiled-coil residues at *d* (and *a*) sites are located at the hydrophobic face that forms the dimerization interface between the helices. Solution quenchers of tryptophan fluorescence have been used extensively to characterize

the location of tryptophans in proteins [8,13,14, 28]. Our quenching study of the tryptophans in the coiled-coil region of myosin (myosin rod) indicates that the bulky tryptophan residues do not fit into this simple coiled-coil structural model.

Our quenching data suggest that there are two physically distinguishable classes of tryptophan in the myosin rod. One is a long lifetime component that is relatively accessible to solvent quenchers (fractional accessibility of about 25%) while the other is a Gaussian distribution of short lifetime components that is relatively inaccessible to solvent quenchers (fractional accessibility of less than 10%). We will discuss the quenching data for iodide, acrylamide, and cesium in light of this model.

The effect of iodide on the fluorescence of rod presents a consistent illustration of the bimodal quenching of tryptophan. The steady-state intensity measurements at high iodide concentration required two quenching constants of 5.3 and 0.31 M^{-1} (with fractional intensities of 0.83 and 0.17, respectively) for an adequate description. The larger quenching constant was similar to the quenching constant of the long lifetime component (4.53 M^{-1}) found from time-resolved measurements while the smaller was within the range estimated for the K_{sv} value of the Gaussian distributed short lifetime component ($\leq 0.4\ M^{-1}$); the distribution of quenching constants (0.83 and 0.17) was also comparable to the distribution of fractional fluorescence intensities for the different lifetime components (0.96 and 0.04 for the long and short lifetime components, respectively, calculated from the lifetimes and fractional distributions).

The quenching behavior of acrylamide was also consistent with this two-component model. The heterogeneity in the steady-state quenching data at high concentrations of acrylamide (Fig. 2B) was well fit using a two component dynamic quenching model with Stern–Volmer constants of 8.38 M^{-1} and $\leq 0.0344\ M^{-1}$. The addition of a static quenching constant term into the analysis (eq. 3) did not improve the quality of the fit; the fit value of the static quenching constant (V) was 0 M^{-1} with large standard deviation (≈ 2–3 M^{-1}). Although static quenching is a phenomenon common in acrylamide quenching of protein fluorescence [29] and apparent in our quenching curves of NATA at high acrylamide concentration (Fig. 2B), there was no direct evidence in our data for static quenching of rod. It is possible, however, that the curvature in the intensity data may reflect the sum of two opposing phenomena, a downward curvature due to heterogeneity and a slight upward curvature due to static quenching. The difference between the Stern–Volmer quenching constant from intensity data ($K_{sv,1} = 8.38\ M^{-1}$) and lifetime data ($K_{sv,1} = 6.18\ M^{-1}$) supports this analysis; the presence of a static quenching component would increase the fit value of $K_{sv,1}$ in the steady-state analysis (compare eqs. 2 and 3). The distribution of quenching constants from the steady-state two component analysis (0.93 and 0.07) was also in remarkable agreement with the distribution of fractional fluorescence intensities (0.96 and 0.04).

The positively charged quencher cesium provided no indication of quenching heterogeneity; this failure is not unexpected given the inefficient nature of the quenching process for this positively charged quencher. The ratio of k_q for rod to that for NATA for cesium, however, indicated that the tryptophans in rod were effectively shielded from this positively charged probe. Such behavior has been seen in other proteins [22] and suggests that the local environment around the rod tryptophans is positively charged. Examination of the sequence around these tryptophans [25] in light of the coiled-coil model confirms that there are multiple lysine and arginine residues in the vicinity of both pairs of tryptophans.

These quenching data demonstrate that the discrete long lifetime component of rod tryptophan fluorescence corresponds to a fraction of solvent accessible tryptophans; this component has a red-shifted emission spectra [3]. The Gaussian distributed short lifetime component, on the other hand, corresponds to a fraction of solvent inaccessible tryptophans; this component has a blue-shifted emission spectra [3]. The tryptophans in the rod thus appear to be in two distinct physical environments. One species has a discrete long lifetime, is in a polar environment, and is accessible to solution quenchers; this species is

partially exposed to aqueous solvent and is thus located near the protein surface. The other species has a Gaussian distribution of short lifetimes, is in a non-polar environment, and is relatively inaccessible to solution quenchers; this species is thus predominantely buried in the protein matrix and is probably located at the coiled-coil interface. The approximate distribution of these components is about 80% exposed and 20% buried.

A detailed physical interpretation of these results is problematic and hinges on the physical origins of the exposed and buried species. Two different extremes of interpretation are possible [3]. One of the tryptophans (i.e. $\approx 25\%$) may be buried all of the time while the remaining three tryptophans are exposed all of the time. Or, all of the tryptophans may be in equilibrium between buried and exposed conformations. Although the symmetry of the protein (rod is a dimer of identical subunits) argues that equivalent tryptophans should be in symmetrical environments, such symmetry arguments may not be relevant to flexible α-helices coiled into a superhelix. A recent NMR study of an *N*-terminal fragment of rod, for example, indicates that equivalent residues in each chain may be in asymmetric environments [30]. At the other extreme, if all of the tryptophans spend 20% of their time in buried and 80% in exposed conformations, then the rod must undergo conformational fluctuations that change the nature of the interactions of the residues at the coiled-coil interface. It is not possible to decide between these two interpretations given the present data.

The fluorescence results clearly indicate that the indole side chains of tryptophan, despite their sequential location at hydrophobic interfacial *d* sites, are not actually located at the coiled-coil interface but are, instead, preferentially exposed to solvent. A recent report of the crystal structure of a synthetic a-helical peptide [31] illuminates our results; this study found that the synthetic protein forms an unusual trimeric coiled-coil bundle with two parallel and one anti-parallel strand. The side chains of the three tryptophans in this protein are displaced from the coiled-coil interface and in contact with solvent. Our combined findings thus cast doubt on the general application of a simple coiled-coil model to describe all coiled-coil interactions in solution and suggest a role for specific, especially bulky residues, in modulating the local coiled-coil interactions.

Acknowledgements

This is publication number D-10115-2-93 of the New Jersey Agricultural Experiment Station. We thank Dr. Scott Williams for expert help in data analysis. This work was supported in part by the State of New Jersey, by a Grant-in-Aid of Research from Sigma Xi, the Scientific Research Society (to Y.-C.C.), and by NIH grant RR01348 to the Regional Laser and Biotechnology Laboratory.

References

1 R.D.B. Fraser and T.P. MacRae, Conformation in fibrous proteins (Academic Press, New York, 1973).
2 C. Cohen and D.A.D. Parry, Proteins 7 (1990) 1.
3 Y.-C. Chang and R.D Ludescher, Biophys. Chem. (1993) submitted.
4 F.H.C. Crick, Acta Crystallogr. 6 (1953) 689.
5 A.D. McLachlan and M. Stewart, J. Mol. Biol. 98 (1975) 293.
6 W.F. Harrington and M. Burke, Biochemistry 11 (1972) 1448.
7 T.M. Eads, D.D. Thomas and R.H. Austin, J. Mol. Biol. 178 (1984) 55.
8 M.R. Eftink, in: Topics in fluorescence spectroscopy, vol. 2: Principles, ed. J.R. Lakowicz (Plenum Press, New York, 1991) p. 53.
9 M.R. Eftink and C.A. Ghiron, J. Phys. Chem. 80 (1976) 486.
10 J.M. Beechem and E. Gratton, Time resolved laser spectroscopy in biochemistry, Proc. SPIE 909 (1988) 70.
11 J.M. Beechem, E. Gratton, M. Ameloot, J.R. Knutson and L. Brand, in: Topics in Fluorescence Spectroscopy, Vol. 2: Principles, ed. J.R. Lakowicz (Plenum Press, New York 1991) p. 241.
12 D.A. Johnson and J. Yguerabide, Biophys. J. 48 (1985) 949.
13 M.R. Eftink and C.A. Ghiron, Anal. Biochem. 114 (1981) 199.
14 S.S. Lehrer, Biochemistry 10 (1971) 3254.
15 W.F. Stafford, Biochemistry 24 (1985) 3314.

16 J.B.A. Ross, C.J. Schmidt and L. Brand, Biochemistry 20 (1981) 4369.
17 L.X.Q. Chen, J.W. Longworth and G.R. Fleming, Biophys. J. 51 (1987) 865.
18 Z. Wayslewski and M.R. Eftink, Biochim. Biophys. Acta 915 (1987) 331.
19 Y.-C. Chang and R.D. Ludescher, Time-Resolved Laser Spectroscopy in Biochemistry III, SPIE Proc. 1640 (1992) 159.
20 R.M. Noyes, Prog. React. Kinet. 1 (1961) 129.
21 A.G. Szabo, and D.M. Rayner, J. Am. Chem. Soc. 102 (1980) 554.
22 R.D. Ludescher, J.J. Volwerk, G.H. de Haas and B.S. Hudson, Biochemistry 24 (1985) 7240.
23 A.D. McLachlan and J. Karn, Nature 299 (1982) 226.
24 R.C. Lu and A. Wong, J. Biol. Chem. 260 (1985) 3456.
25 K. Maeda, G. Sczakiel and A. Wittinghofer, Eur. J. Biochem. 167 (1987) 97.
26 L. Pauling and R.B. Corey, Nature 171 (1953) 59.
27 E.K. O'Shea, J.D. Klemm, P.S. Kim and T. Alber, Science 254 (1991) 539.
28 S.S. Lehrer, Biochem. Biophys. Res. Commun. 29 (1967) 767.
29 K.A. Hagaman and M.R. Eftink, Biophys. Chem. 20 (1984) 201.
30 H.R. Kalbitzer, K. Maeda, A. Rosch, Y. Maeda, M. Geyer, W. Beneicke, K.P. Neidig and A. Wittinghofer, Biochemistry 30 (1991) 8083.
31 B. Lovejoy, S. Choe, D. Cascio, D.K. McRoie, W.F. DeGrado and D. Eisenberg, Science 259 (1993) 1288.